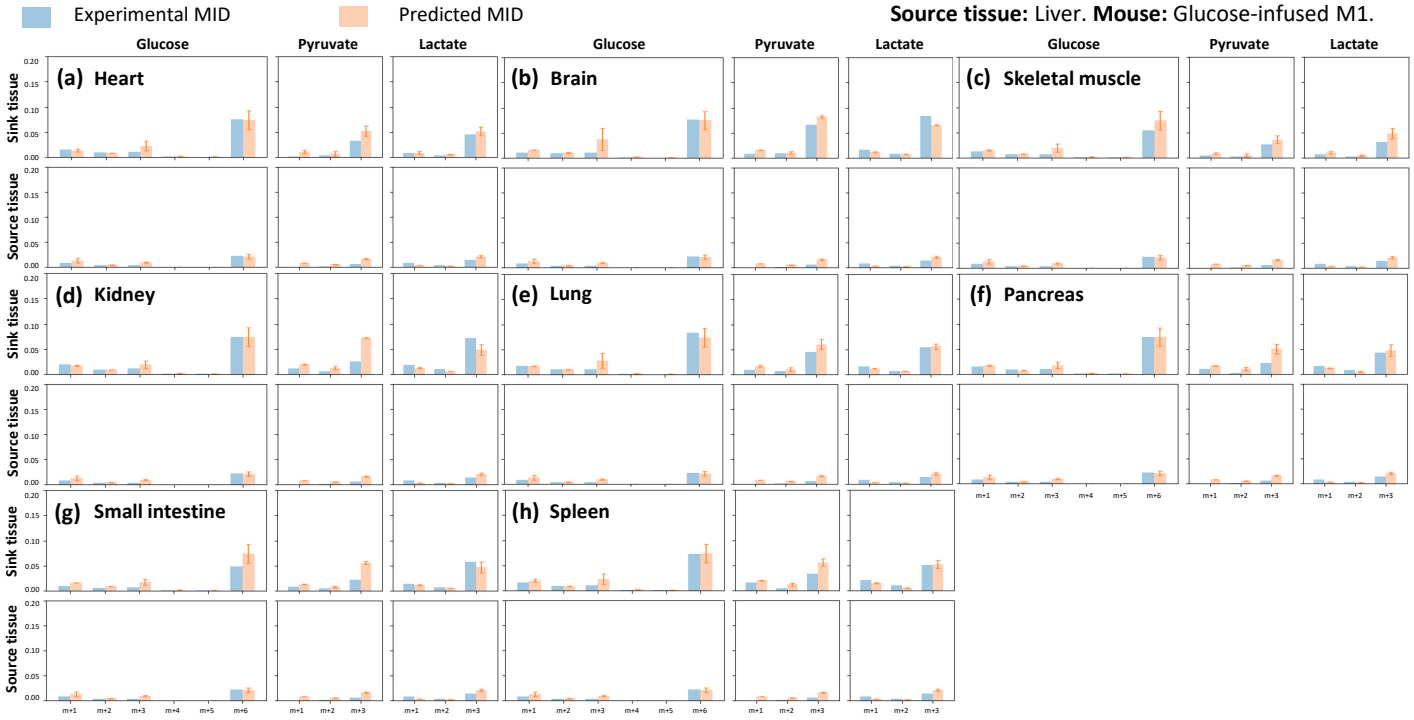
Experimental MID
Predicted MID
Source tissue: Liver. Mouse: Glucose-infused M1.
Glucose
Pyruvate
Lactate
(a) Heart
(b) Brain
(c) Skeletal muscle
(d) Kidney
(e) Lung
(f) Pancreas
(g) Small intestine
(h) Spleen
Sink tissue
Source tissue

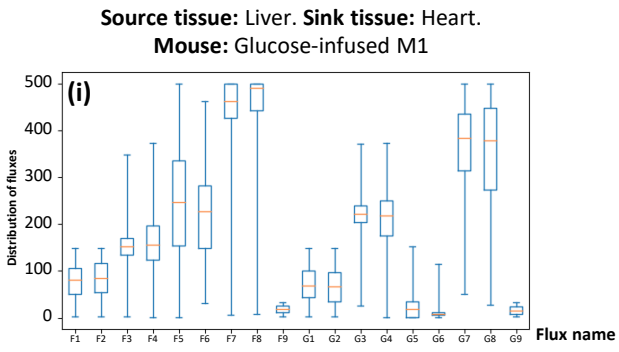
Source tissue: Liver. Sink tissue: Heart.
Mouse: Glucose-infused M1
(i)
Distribution of fluxes
Flux name
F1 F2 F3 F4 F5 F6 F7 F8 F9 G1 G2 G3 G4 G5 G6 G7 G8 G9

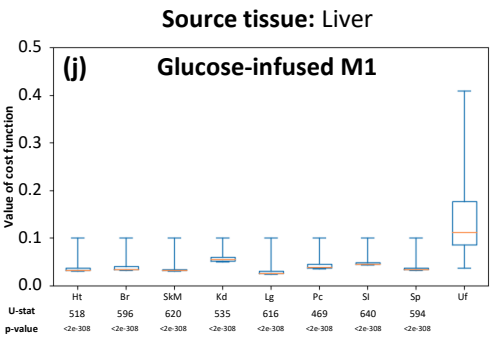
Source tissue: Liver
(j) Glucose-infused M1
Value of cost function
Ht Br SkM Kd Lg Pc Sl Sp Uf
U-stat 518 596 620 535 616 469 640 594
p-value <2e-308

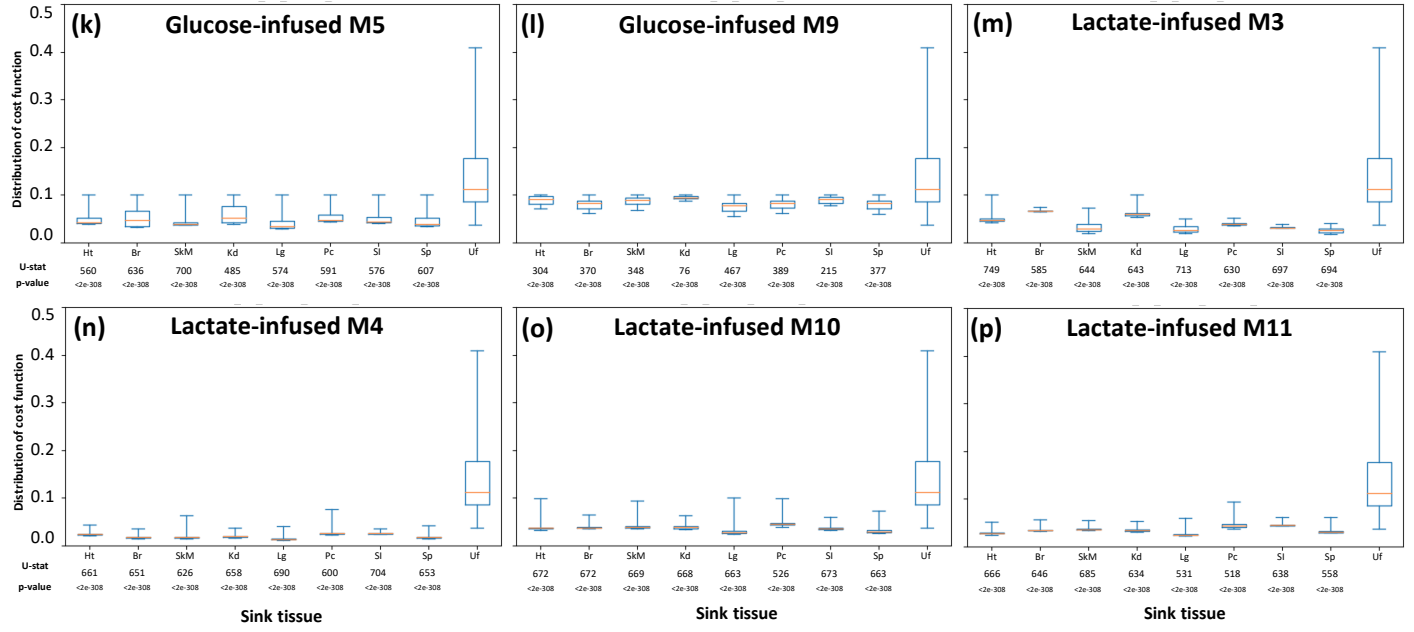
(k) Glucose-infused M5
(l) Glucose-infused M9
(m) Lactate-infused M3
(n) Lactate-infused M4
(o) Lactate-infused M10
(p) Lactate-infused M11
Distribution of cost function
Ht Br SkM Kd Lg Pc Sl Sp Uf
U-stat
p-value
Sink tissue

Figure S1. Detailed information of model fitting. Related to Figure 1.

(a-h) Comparison of experimental and predicted MID in the model. Average values of predicted MID in all feasible solutions are displayed. Standard deviation is also displayed as error bar. In most cases, the experimental MID is captured by this model. Because of the low abundance of labeled isotopomers, only isotopomers with more than one ^{13}C are displayed. **(i)** Distribution of 18 variable fluxes in all feasible solutions. Source tissue is liver and sink tissue is heart. **(j-p)** Distribution of cost functions of feasible solutions fitted with different sink tissue and data from different mice, compared with unfitted control data. Source tissue in all fittings is liver. U-statistics of rank-sum test and p-values are displayed.

In all subfigures, fits are based on mice from the low-infusion data in Hui et al, 2017, and source tissue is liver. Specifically, subfigures **(a-h)** and **(i)** are fitted with glucose-infused mouse M1. The sink tissue in **(i)** is heart. In all box plots, boxes represent quantiles and whiskers represent extremes. Ht: heart, Br: brain, SkM: skeletal muscle, Kd: kidney, Lg: lung, Pc: pancreas, SI: small intestine, Sp: spleen, Uf: data from random unfitted control.

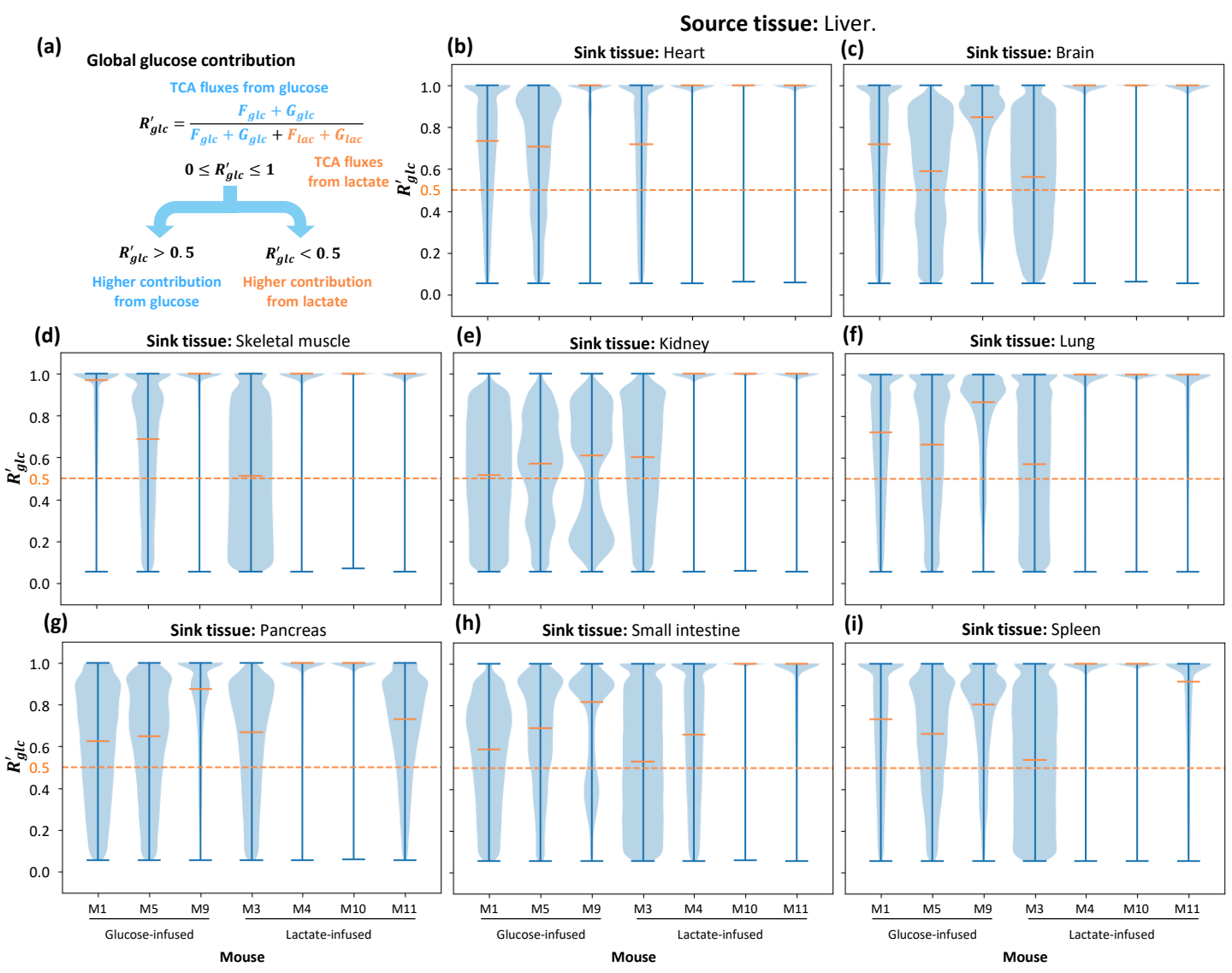
Source tissue: Liver.
(a)
Global glucose contribution
TCA fluxes from glucose
$R'_{glc} = \frac{F_{glc} + G_{glc}}{F_{glc} + G_{glc} + F_{lac} + G_{lac}}$
$0 \le R'_{glc} \le 1$
TCA fluxes from lactate
$R'_{glc} > 0.5$
$R'_{glc} < 0.5$
Higher contribution from glucose
Higher contribution from lactate
(b) Sink tissue: Heart
(c) Sink tissue: Brain
(d) Sink tissue: Skeletal muscle
(e) Sink tissue: Kidney
(f) Sink tissue: Lung
(g) Sink tissue: Pancreas
(h) Sink tissue: Small intestine
(i) Sink tissue: Spleen
R'_{glc}
1.0
0.8
0.6
0.5
0.4
0.2
0.0
M1 M5 M9 M3 M4 M10 M11
Glucose-infused
Lactate-infused
Mouse

Figure S2. The global contribution ratio from circulating glucose to the TCA cycle. Related to Figure 2.

(a) Definition of global glucose contribution ratio in complete model R'_{glc}. The global contribution R'_{glc} is defined as the relative ratio of glucose contribution flux to total contribution flux in sink and source tissue. Similar with R_{glc}, this contribution is also a scalar between 0 and 1. Higher R'_{glc} represents an increasing glucose contribution to the TCA cycle. **(b-i)** Distribution of glucose contribution in complete model based on the model with different sink tissues. For each sink tissue, the source tissue is liver and contribution ratio is calculated from data in 7 different mice. Similar with results with R_{glc}, for most kinds of sink tissue, the median of global glucose contribution R'_{glc} is close to or higher than 0.5 in most mice, which means glucose contributes more than lactate to the TCA cycle in complete model. The orange dash line represents 0.5 threshold. Data set is from glucose-infused mice (M1, M5, M9) and lactate-infused mice (M3, M4, M10, M11) in Hui et al, Nature 2017.

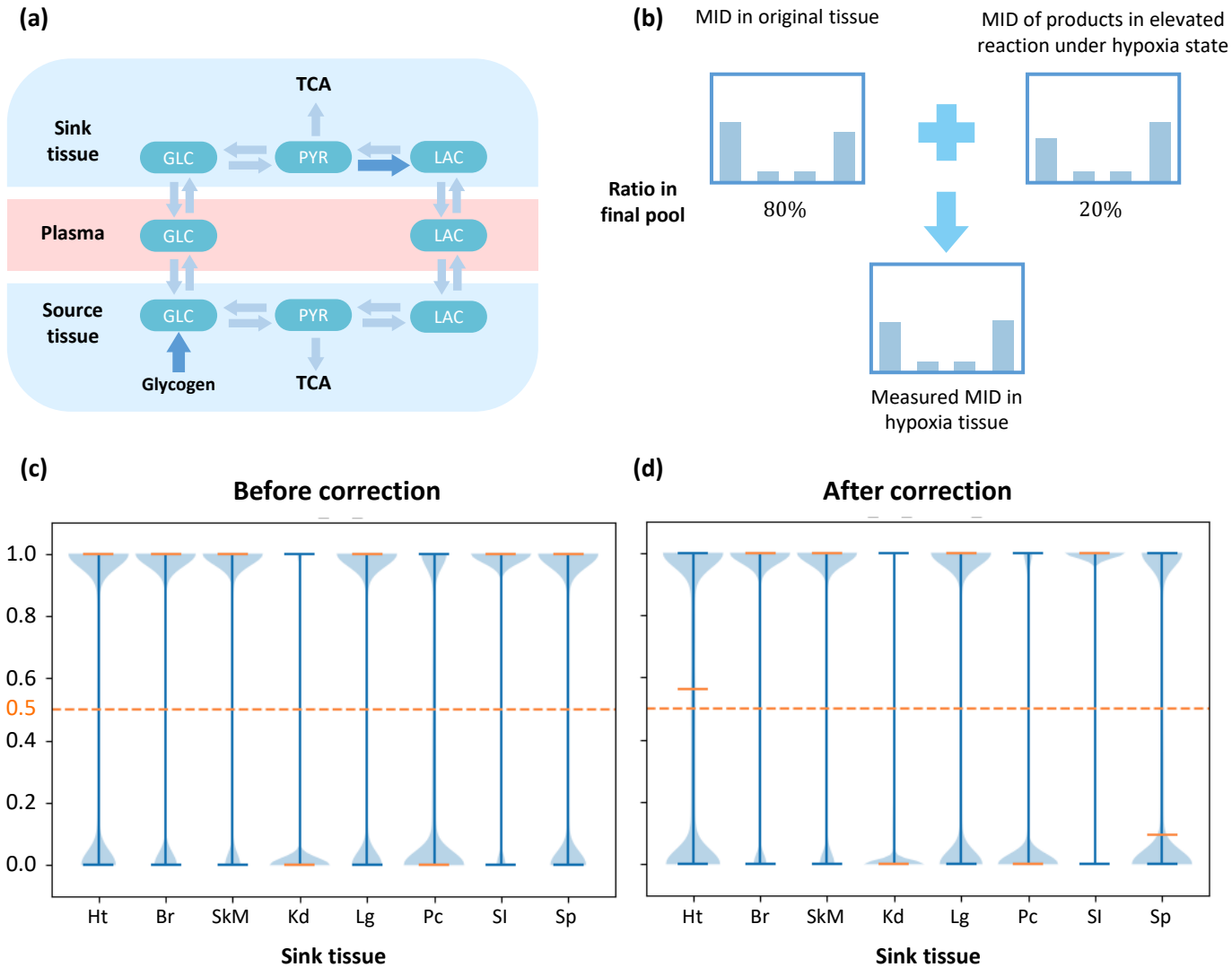

Source tissue: Liver

Mouse: Glucose-infused M1

Figure S3. Distribution of local glucose contribution under hypoxia correction. Related to Figure 3.

(a) Two possible elevated fluxes under hypoxia. **(b)** Final measured MID is regarded as mixture of MIDs from real metabolite and products in elevated reaction under hypoxia state. **(c-d)** Distribution of local glucose contribution before **(c)** or after **(d)** correction. Model is fitted with data from mouse M1 in data from Hui et al Nature 2017. Sink tissue is liver. Ht: heart, Br: brain, SkM: skeletal muscle, Kd: kidney, Lg: lung, Pc: pancreas, SI: small intestine, Sp: spleen.

(a)

Source tissue: Liver. **Sink tissue:** Skeletal muscle. **Data:** High-infusion data. **Mouse:** Glucose-infused M1.

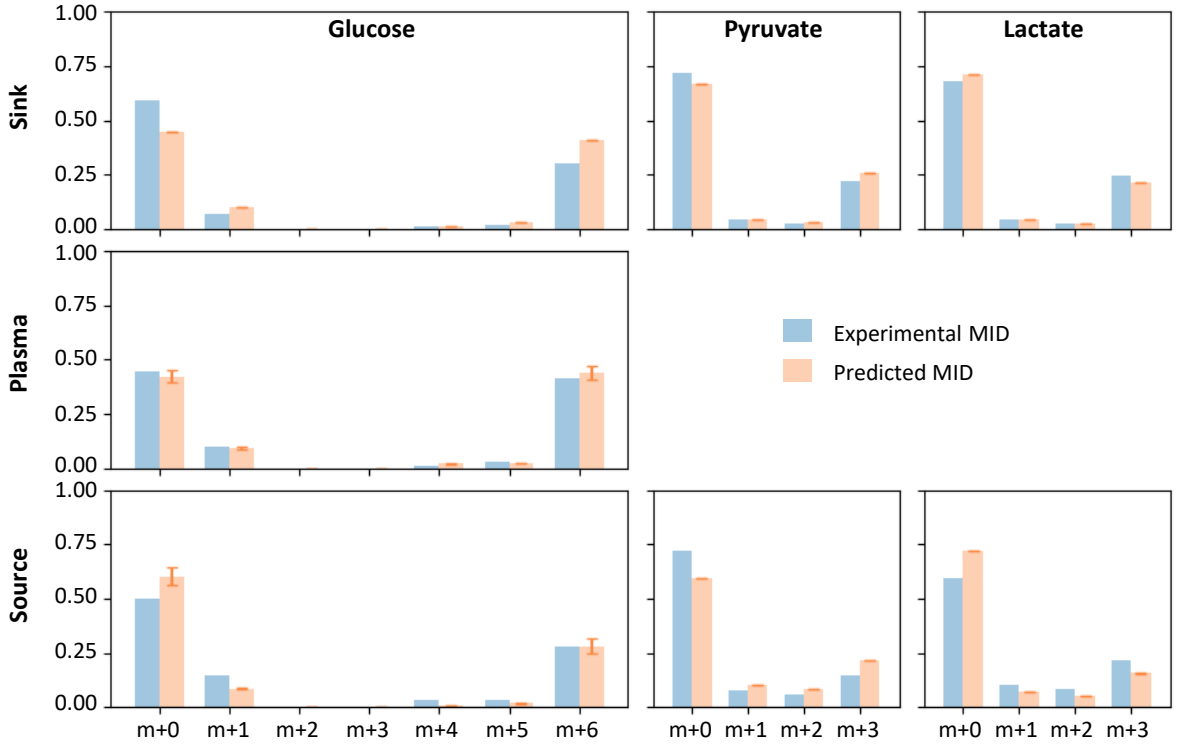

(b)

Source tissue: Liver. **Sink tissue:** Skeletal muscle. **Data:** High-infusion data.

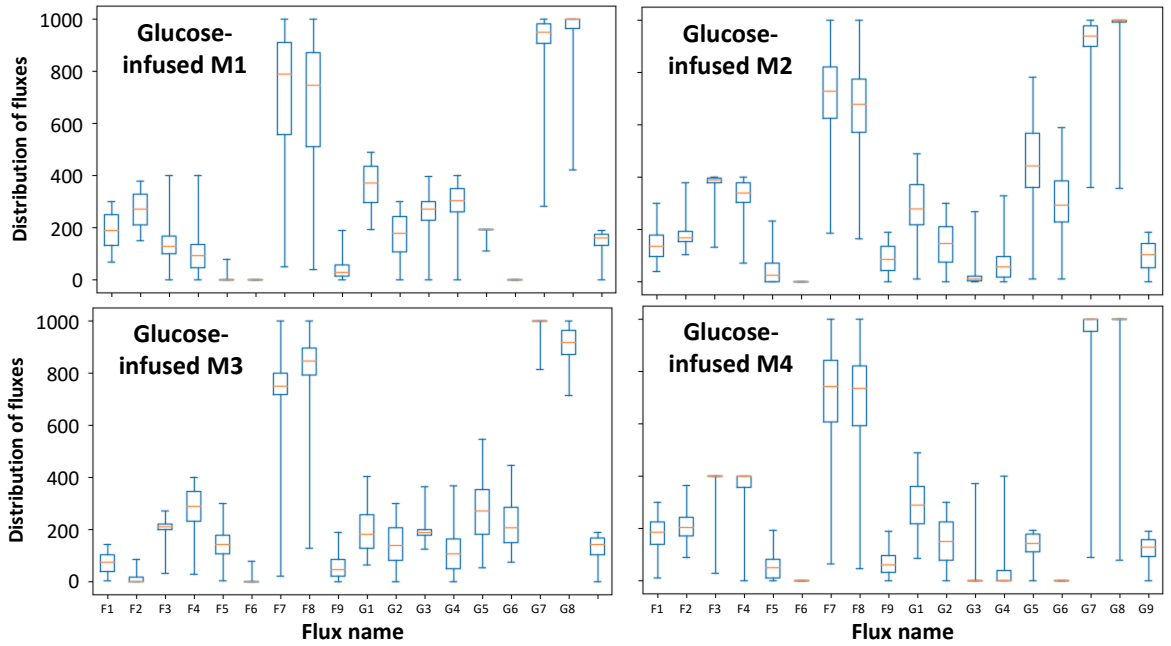

(c)

Global glucose contribution

$$R'_{glc} = \frac{F_{glc} + G_{glc}}{F_{glc} + G_{glc} + F_{lac} + G_{lac}}$$

TCA fluxes from glucose

TCA fluxes from lactate

Source tissue:	Liver
Sink tissue:	Skeletal muscle
Data:	High-infusion data

(d)

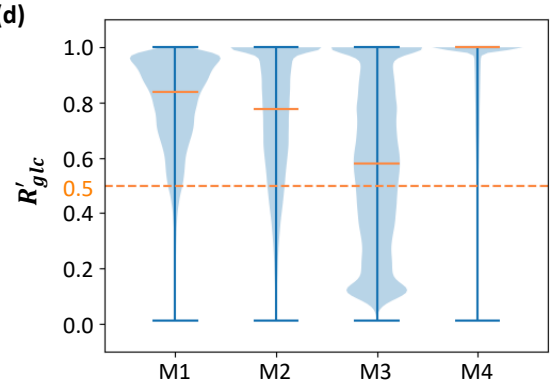

Figure S4. Detailed information for the high-infusion system. Related to Figure 4.

(a) Comparison of experimental and predicted MID in the model. Average of predicted MID in all feasible solutions are displayed. Standard deviation is also displayed as error bar. Experimental MID could be well predicted by this model. Notably, the ratio of high ^{13}C isotopomer is significantly higher than that of the original system. **(b)** Distribution of 18 variable fluxes in all feasible solutions. **(c)** Definition of global glucose contribution in complete model R'_{glc}. The global glucose contribution R'_{glc} is defined as the relative ratio of glucose contribution flux to total contribution flux in sink and source tissue. **(d)** Similar with results with local contribution R_{glc}, distribution of global glucose contribution in complete model R'_{glc} shows glucose contributes more than lactate to the TCA cycle in all mice. Fittings from different mice are displayed.

In all subfigures, the fitting is based on different glucose-infused mice from the high-infusion data. Source tissue is liver and sink tissue is skeletal muscle. Specifically, subfigure **(a)** is based on data from glucose-infused mouse M1. In all box plots, boxes represent quantiles and whiskers represent extremes.

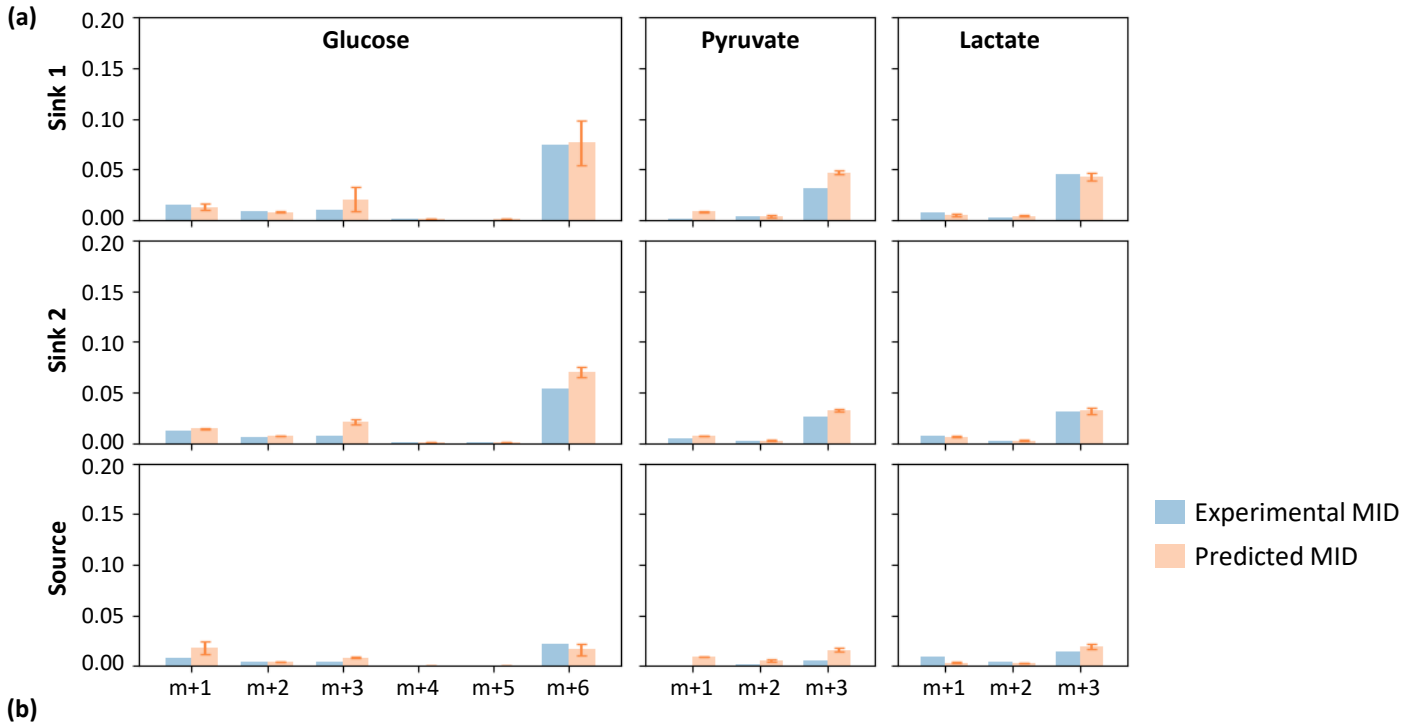
(a)
Glucose
Pyruvate
Lactate
Sink 1
Sink 2
Source
0.20
0.15
0.10
0.05
0.00
m+1
m+2
m+3
m+4
m+5
m+6
Experimental MID
Predicted MID

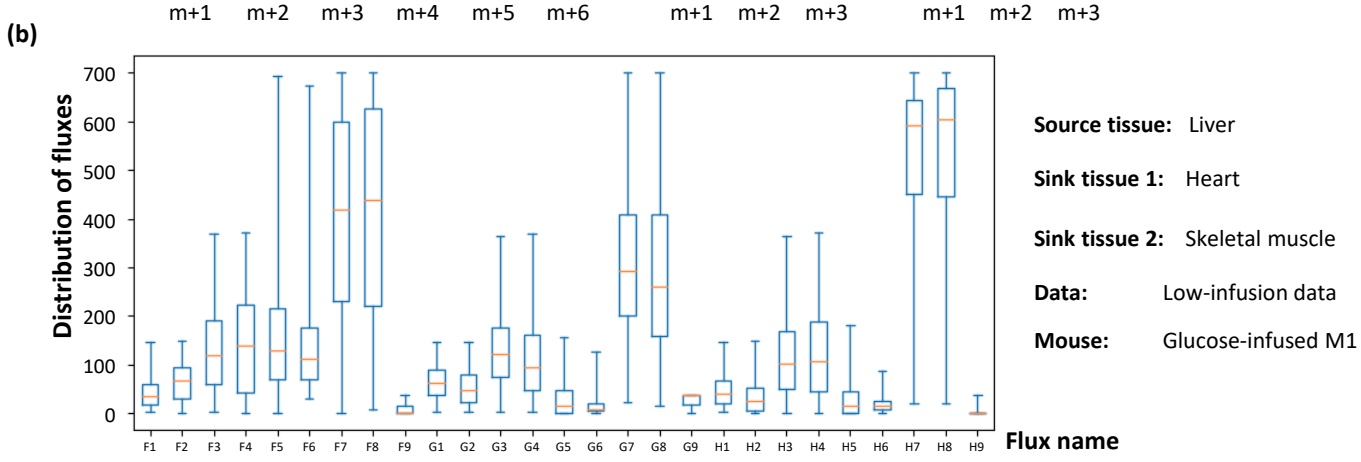
(b)
Distribution of fluxes
700
600
500
400
300
200
100
0
F1 F2 F3 F4 F5 F6 F7 F8 F9 G1 G2 G3 G4 G5 G6 G7 G8 G9 H1 H2 H3 H4 H5 H6 H7 H8 H9
Flux name
Source tissue: Liver
Sink tissue 1: Heart
Sink tissue 2: Skeletal muscle
Data: Low-infusion data
Mouse: Glucose-infused M1

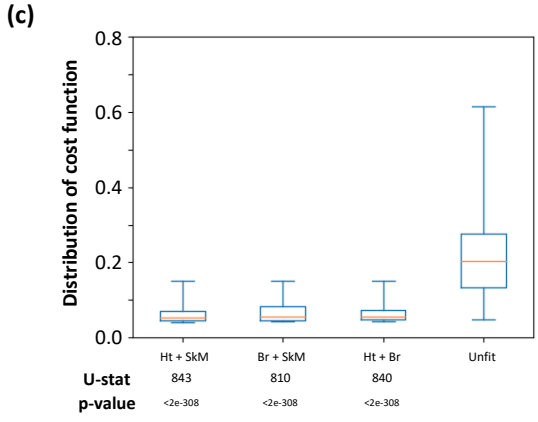
(c)
Distribution of cost function
0.8
0.6
0.4
0.2
0.0
Ht + SkM
Br + SkM
Ht + Br
Unfit
U-stat
843
810
840
p-value
<2e-308
<2e-308
<2e-308

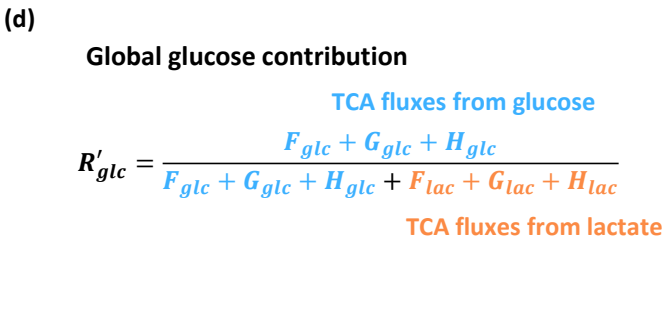
(d)
Global glucose contribution
TCA fluxes from glucose
$R'_{glc} = \frac{F_{glc} + G_{glc} + H_{glc}}{F_{glc} + G_{glc} + H_{glc} + F_{lac} + G_{lac} + H_{lac}}$
TCA fluxes from lactate

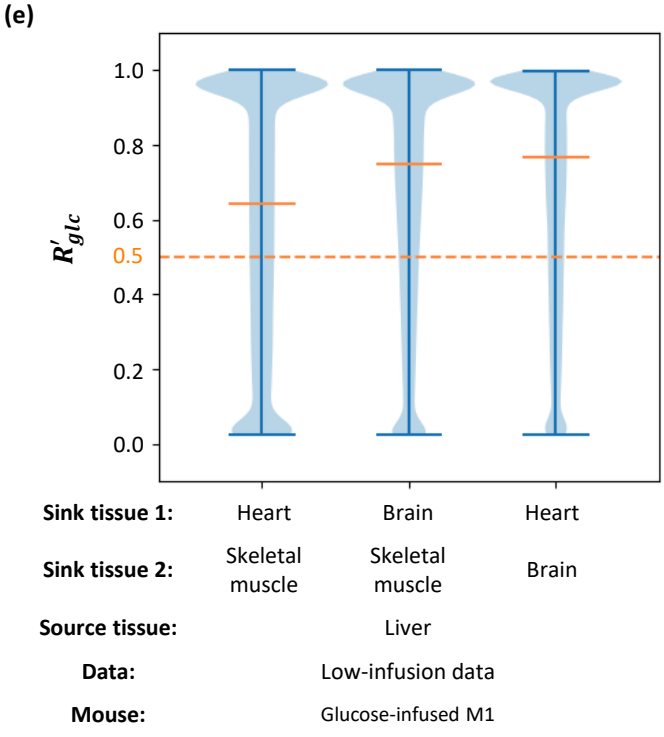
(e)
R'_{glc}
1.0
0.8
0.6
0.5
0.4
0.2
0.0
Sink tissue 1: Heart Brain Heart
Sink tissue 2: Skeletal muscle Skeletal muscle Brain
Source tissue: Liver
Data: Low-infusion data
Mouse: Glucose-infused M1

Figure S5. Detailed information of the multi-tissue model. Related to Figure 5.

(a) Comparison of experimental and predicted MID in the model. Average of predicted MID in all feasible solutions are displayed. Standard deviation is also displayed as error bar. Experimental MID could be well predicted by this model. Because of the low abundance, only isotopomers with more than one ^{13}C are displayed. **(b)** Distribution of 27 variable fluxes in all feasible solutions. **(c)** Distribution of cost functions of feasible solutions compared with that from unfitted control. U-statistics of rank-sum test and p-values are displayed. **(d)** Definition of global glucose contribution in complete model R'_{glc}. This global contribution R'_{glc} is defined as the relative ratio of glucose contribution flux to total contribution flux in all three kinds of tissue. **(e)** Similar with results with local contribution R_{glc}, distribution of global glucose contribution in complete model R'_{glc} shows glucose contributes more than lactate to the TCA cycle in all combinations of sink tissue.

In all subfigures, the model is fitted with glucose-infused mouse M1 from the low-infusion data in Hui et al, 2017. The source tissue is liver and the sink tissue 1 and 2 are two from heart, brain and skeletal muscle respectively. In all box plots, boxes represent quantiles and whiskers represent extremes.

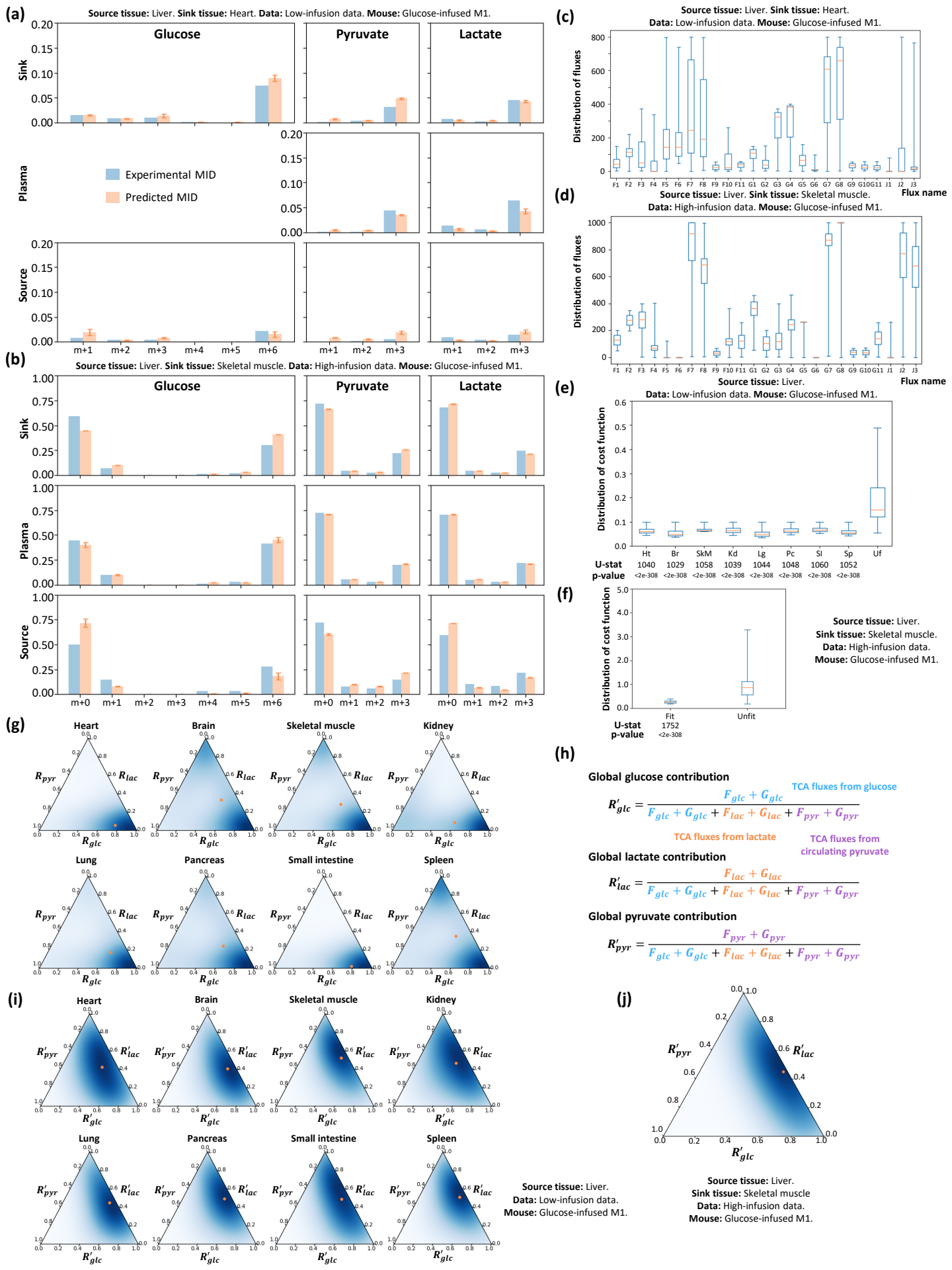
(a)
Source tissue: Liver. Sink tissue: Heart. Data: Low-infusion data. Mouse: Glucose-infused M1.
Glucose
Pyruvate
Lactate
Sink
Plasma
Source
Experimental MID
Predicted MID
m+1 m+2 m+3 m+4 m+5 m+6
(b)
Source tissue: Liver. Sink tissue: Skeletal muscle. Data: High-infusion data. Mouse: Glucose-infused M1.
m+0 m+1 m+2 m+3 m+4 m+5 m+6
(c)
Source tissue: Liver. Sink tissue: Heart.
Data: Low-infusion data. Mouse: Glucose-infused M1.
Distribution of fluxes
F1 F2 F3 F4 F5 F6 F7 F8 F9 F10 F11 G1 G2 G3 G4 G5 G6 G7 G8 G9 G10 G11 J1 J2 J3
Flux name
(d)
Source tissue: Liver. Sink tissue: Skeletal muscle.
Data: High-infusion data. Mouse: Glucose-infused M1.
(e)
Source tissue: Liver.
Data: Low-infusion data. Mouse: Glucose-infused M1.
Distribution of cost function
Ht Br SkM Kd Lg Pc Sl Sp Uf
U-stat 1040 1029 1058 1039 1044 1048 1060 1052
p-value <2e-308
(f)
Distribution of cost function
Fit Unfit
U-stat 1752
p-value <2e-308
Source tissue: Liver.
Sink tissue: Skeletal muscle.
Data: High-infusion data.
Mouse: Glucose-infused M1.
(g)
Heart Brain Skeletal muscle Kidney
Lung Pancreas Small intestine Spleen
R_{pyr} R_{lac} R_{glc}
(h)
Global glucose contribution
$$R'_{glc} = \frac{F_{glc} + G_{glc}}{F_{glc} + G_{glc} + F_{lac} + G_{lac} + F_{pyr} + G_{pyr}}$$
TCA fluxes from glucose
TCA fluxes from lactate
TCA fluxes from circulating pyruvate
Global lactate contribution
$$R'_{lac} = \frac{F_{lac} + G_{lac}}{F_{glc} + G_{glc} + F_{lac} + G_{lac} + F_{pyr} + G_{pyr}}$$
Global pyruvate contribution
$$R'_{pyr} = \frac{F_{pyr} + G_{pyr}}{F_{glc} + G_{glc} + F_{lac} + G_{lac} + F_{pyr} + G_{pyr}}$$
(i)
Heart Brain Skeletal muscle Kidney
Lung Pancreas Small intestine Spleen
R'_{pyr} R'_{lac} R'_{glc}
Source tissue: Liver.
Data: Low-infusion data.
Mouse: Glucose-infused M1.
(j)
Source tissue: Liver.
Sink tissue: Skeletal muscle
Data: High-infusion data.
Mouse: Glucose-infused M1.

Figure S6. Detailed information of the model with multiple circulating metabolites. Related to Figure 6.

(a, b) Comparison of experimental and predicted MID in the model fitted with the low-infusion data **(a)** or the high-infusion data **(b)**. Average of predicted MID in all feasible solutions are displayed. Standard deviation is also displayed as error bar. Experimental MID could be well predicted by this model. **(c, d)** Distribution of 25 variable fluxes in all feasible solutions fitted with the low-infusion data **(c)** or the high-infusion data **(d)**. **(e, f)** Distribution of cost functions of feasible solutions compared with that from random unfitted control, fitted with the low-infusion data **(e)** or the high-infusion data **(f)**. U-statistics of rank-sum test and p-values are displayed. **(g)** Local contributions to the TCA cycle when additional nutrients are considered. For most sink tissues, glucose contributes to the TCA cycle more than lactate and pyruvate, especially in heart, kidney, lung, and small intestine. The orange point indicates average level. **(h)** Definition of global contribution from metabolites in complete model R'_{glc}, R'_{lac} and R'_{pyr}. The three global contribution ratios R'_{glc}, R'_{lac} and R'_{pyr} are defined by the relative ratio of the contribution flux from each metabolite to total contribution flux of all three metabolites in sink and source tissue. **(i)** Ternary plot to display distribution of three contributions R'_{glc}, R'_{lac} and R'_{pyr}. The orange point indicates average level. **(j)** Analysis and results as in **(i)** but for additional high-infusion system of different animal strain, different diet and different infusion protocol.

Subfigure **(a)**, **(c)**, **(e)**, **(g)** and **(i)** are fitted with glucose-infused mouse M1 from the low-infusion data in Hui et al, Nature 2017, and source tissue is liver. Specifically, sink tissue in **(a)** and **(c)** is heart. Subfigure **(b)**, **(d)**, **(f)** and **(j)** are fitted with glucose-infused mouse M1 from the high-infusion data, and the sink tissue and source tissue are liver and skeletal muscle respectively.

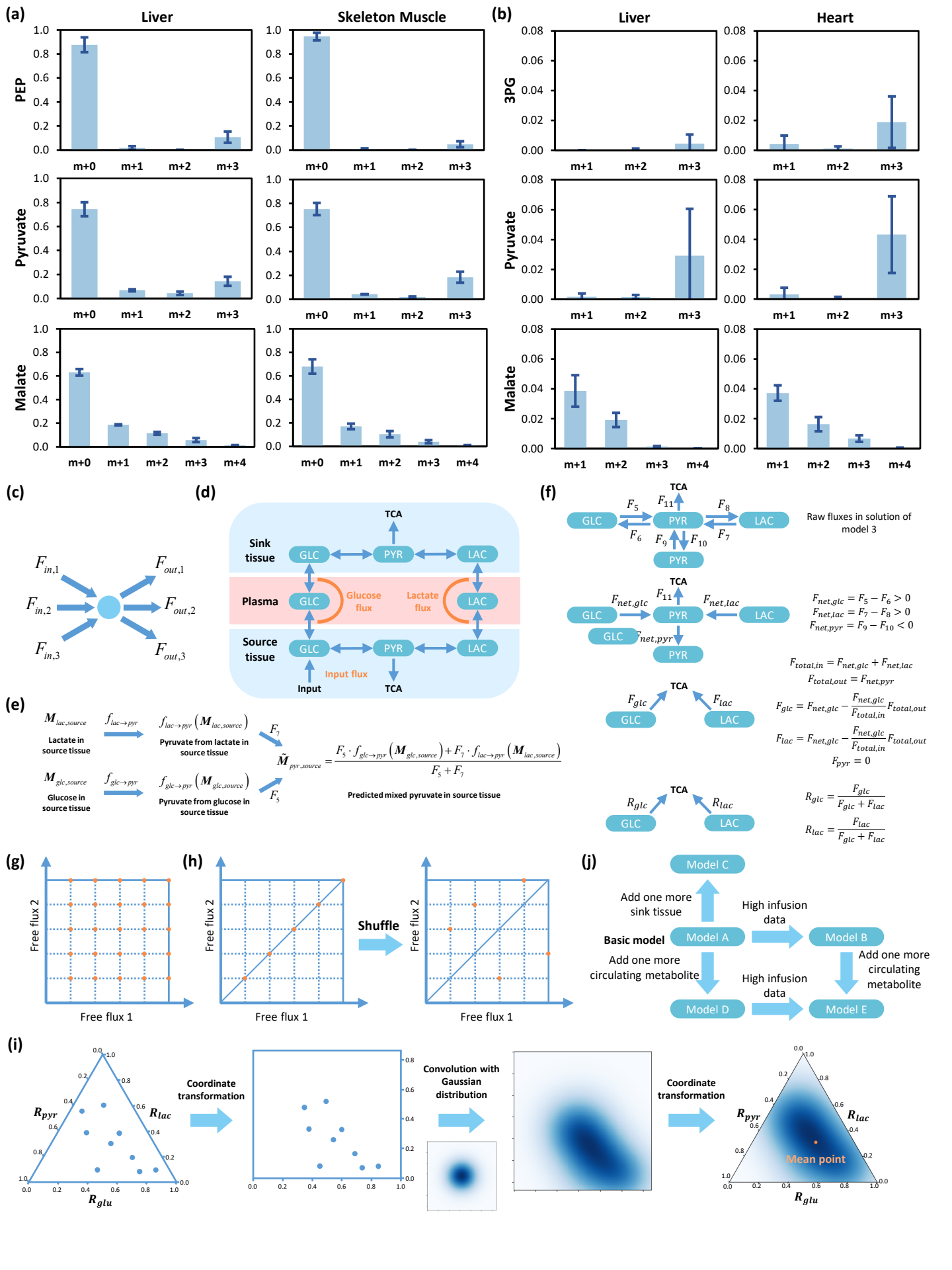
(a)
Liver
Skeleton Muscle
PEP
Pyruvate
Malate
m+0
m+1
m+2
m+3
m+4
(b)
Liver
Heart
3PG
Pyruvate
Malate
(c)
$F_{in,1}$
$F_{in,2}$
$F_{in,3}$
$F_{out,1}$
$F_{out,2}$
$F_{out,3}$
(d)
TCA
Sink tissue
Plasma
Source tissue
GLC
PYR
LAC
Glucose flux
Lactate flux
Input flux
Input
(e)
$M_{lac,source}$
Lactate in source tissue
$f_{lac\to pyr}$
$f_{lac\to pyr}(M_{lac,source})$
Pyruvate from lactate in source tissue
$M_{glc,source}$
Glucose in source tissue
$f_{glc\to pyr}$
$f_{glc\to pyr}(M_{glc,source})$
Pyruvate from glucose in source tissue
F_7
F_5
$\tilde{M}_{pyr,source} = \frac{F_5 \cdot f_{glc\to pyr}(M_{glc,source}) + F_7 \cdot f_{lac\to pyr}(M_{lac,source})}{F_5 + F_7}$
Predicted mixed pyruvate in source tissue
(f)
Raw fluxes in solution of model 3
$F_{net,glc} = F_5 - F_6 > 0$
$F_{net,lac} = F_7 - F_8 > 0$
$F_{net,pyr} = F_9 - F_{10} < 0$
$F_{total,in} = F_{net,glc} + F_{net,lac}$
$F_{total,out} = F_{net,pyr}$
$F_{glc} = F_{net,glc} - \frac{F_{net,glc}}{F_{total,in}} F_{total,out}$
$F_{lac} = F_{net,glc} - \frac{F_{net,glc}}{F_{total,in}} F_{total,out}$
$F_{pyr} = 0$
$R_{glc} = \frac{F_{glc}}{F_{glc} + F_{lac}}$
$R_{lac} = \frac{F_{lac}}{F_{glc} + F_{lac}}$
(g)
Free flux 1
Free flux 2
(h)
Shuffle
(j)
Model C
Add one more sink tissue
Basic model
Model A
High infusion data
Model B
Add one more circulating metabolite
Add one more circulating metabolite
High infusion data
Model D
Model E
(i)
R_{pyr}
R_{lac}
R_{glu}
Coordinate transformation
Convolution with Gaussian distribution
Coordinate transformation
Mean point

Figure S7. Schematics of model design and computations. Related to STAR Methods.

(a, b) MID data of metabolites. Error bars indicate standard deviations. **(a)** MID of 3PG, pyruvate and malate in liver and heart in glucose-infused data from Hui et al Nature 2017. Data for 3PG and malate were collected from 5 mice (labeled as M1, M4, M5, M7 and M9 in their experiments), while those for pyruvate were collected from 3 mice (M1, M5 and M9. Data for pyruvate M4 and M7 were not available). Only non-m+0 isotopomers are plotted because of low abundance. **(b)** MID of PEP, pyruvate and malate in liver and skeleton muscle in glucose-infused data from our high-infusion experiments. Data were collected from 4 mice. **(c)** Diagram of flux balance requirement. Sum of all input fluxes should be the same as sum of all output fluxes. **(d)** Constraints for some fluxes are shown in orange text. "Glucose flux sum" shows the sum of two glucose export fluxes from tissues to plasma, while "lactate flux sum" shows sum of lactate fluxes. "Input flux" shows the fixed incoming glucose flux. **(e)** Diagram of MID prediction. MIDs of substrate metabolites $\boldsymbol{M}_{glc,source}$ and $\boldsymbol{M}_{lac,source}$ are converted to MID of pyruvate by $f_{glc\to pyr}$ and $f_{lac\to pyr}$ respectively. The final MID of pyruvate is predicted based on mixture of two sources, proportional to fluxes F_5 and F_7. **(f)** Calculation of the contribution nutrients to the TCA cycle. From top to bottom are: (1) Suppose there is a one-tissue model, glucose, lactate and pyruvate can all contribute to TCA cycle. (2) Raw fluxes are first converted to net fluxes, which could be positive or negative. (3) Net fluxes are converted to contribution fluxes, which are non-negative. (4) Contribution fluxes are normalized to the calculate contribution ratio for each metabolite. **(g-h)** Two sampling strategies on a two dimensional flux space. **(g)** Uniformly scan the whole space when the dimension of free fluxes is small. **(h)** In high-dimension space, points on diagonal are selected uniformly, then their coordinates are shuffled to generate sample of free fluxes. **(i)** The density distribution of contribution from glucose, lactate and pyruvate. The contribution triple set $\left(R_{glc}, R_{lac}, R_{pyr}\right)$ is first transformed to Cartesian system $\mathbb{R}^2$, and convolved with a Gaussian kernel. Then, the resulting distribution is mapped back to ternary system $\mathbb{T}$ with mean value calculated. **(j)** Relationships between different models. Model A is the basic model. Model C is the model A with one more sink tissue. Model B is the model A fitted with high infusion data. Model D is the model A with one more circulating metabolite (pyruvate), while model E is the model D fitted with high infusion data.

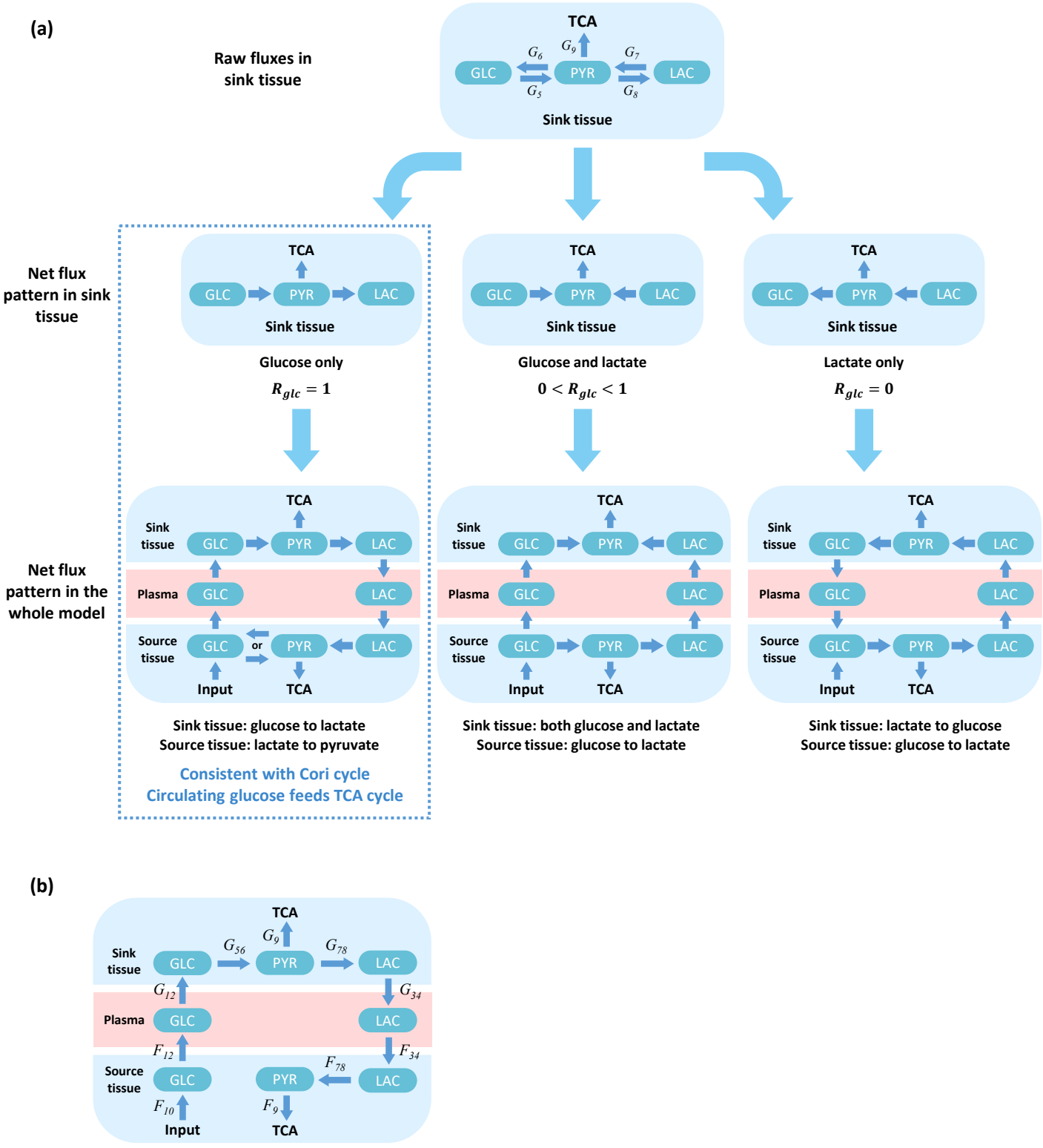
(a)
Raw fluxes in sink tissue
TCA
GLC
PYR
LAC
G_5
G_6
G_7
G_8
G_9
Sink tissue
Net flux pattern in sink tissue
Glucose only
$R_{glc} = 1$
Glucose and lactate
$0 < R_{glc} < 1$
Lactate only
$R_{glc} = 0$
Net flux pattern in the whole model
Sink tissue
Plasma
Source tissue
or
Input
Sink tissue: glucose to lactate
Source tissue: lactate to pyruvate
Consistent with Cori cycle
Circulating glucose feeds TCA cycle
Sink tissue: both glucose and lactate
Source tissue: glucose to lactate
Sink tissue: lactate to glucose
Source tissue: glucose to lactate
(b)
G_{56}
G_{78}
G_{12}
G_{34}
F_{12}
F_{34}
F_{78}
F_{10}
F_9

Figure S8. Distribution of the local glucose contribution R_{glc} and global glucose contribution R'_{glc}. Related to STAR Methods.

(a) Three possible patterns of feasible solutions in our model, which correspond to three glucose contribution ratios: $R_{glc} = 1$, $0 < R_{glc} < 1$ or $R_{glc} = 0$. In the first pattern, glucose is transformed to lactate in sink tissue and lactate is transformed to pyruvate or glucose, which is consistent with Cori cycle. In our results R_{glc} concentrates on 1 supports our conclusion that circulating glucose feeds TCA cycle in most kinds of sink tissue. **(b)** A special case to show how fluxes in this model affect final value of R'_{glc}. Only net fluxes are displayed. In this pattern, if $F9 > G9$, even though all TCA flux in sink tissue derives from circulating glucose, $R'_{glc} < 0.5$.

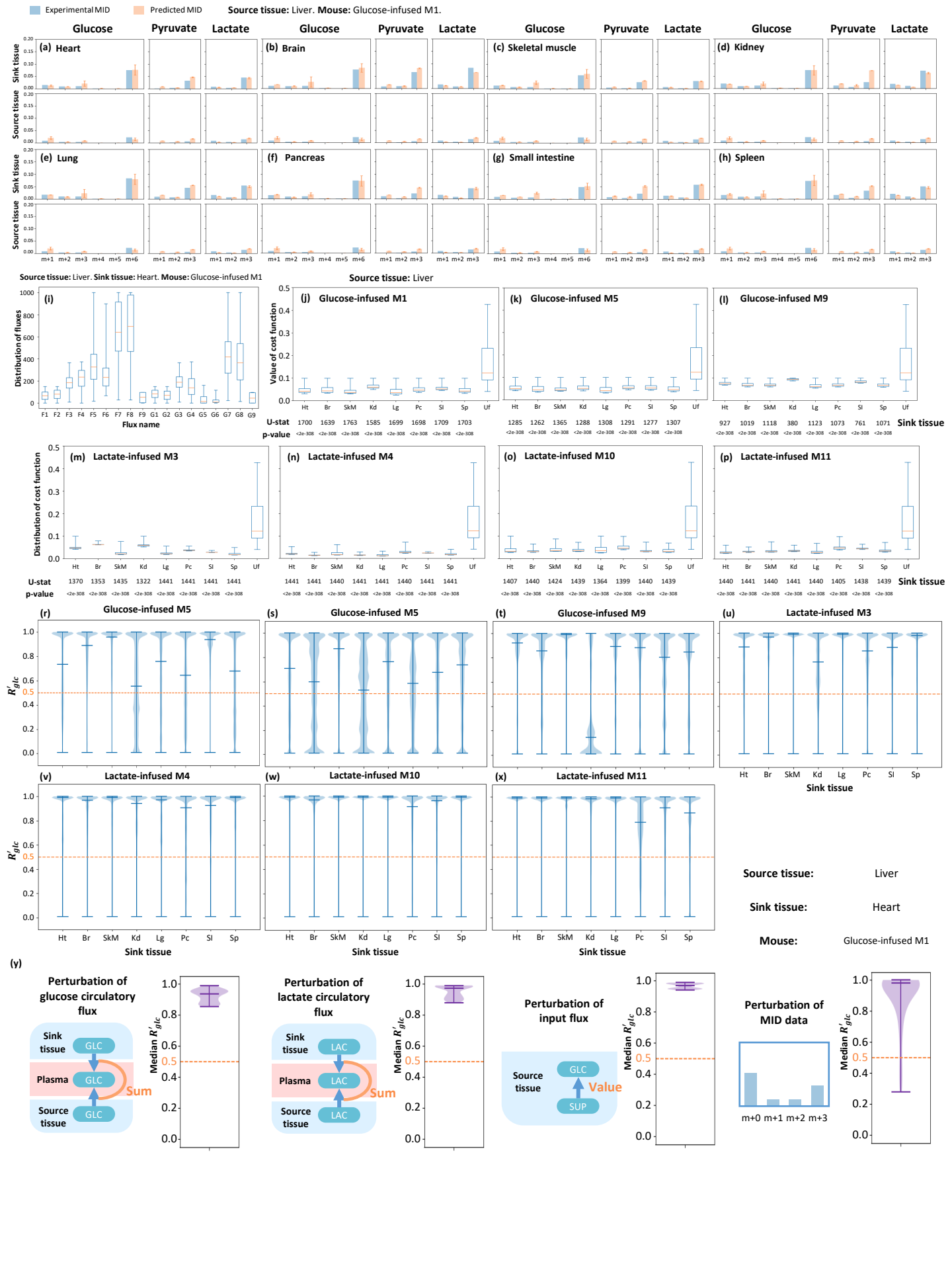
Experimental MID
Predicted MID
Source tissue: Liver. Mouse: Glucose-infused M1.
Glucose
Pyruvate
Lactate
(a) Heart
(b) Brain
(c) Skeletal muscle
(d) Kidney
(e) Lung
(f) Pancreas
(g) Small intestine
(h) Spleen
Sink tissue
Source tissue
m+1 m+2 m+3 m+4 m+5 m+6
Source tissue: Liver. Sink tissue: Heart. Mouse: Glucose-infused M1
(i)
Distribution of fluxes
F1 F2 F3 F4 F5 F6 F7 F8 F9 G1 G2 G3 G4 G5 G6 G7 G8 G9
Flux name
Source tissue: Liver
(j) Glucose-infused M1
(k) Glucose-infused M5
(l) Glucose-infused M9
Value of cost function
Ht Br SkM Kd Lg Pc Sl Sp Uf
U-stat
p-value
Sink tissue
(m) Lactate-infused M3
(n) Lactate-infused M4
(o) Lactate-infused M10
(p) Lactate-infused M11
Distribution of cost function
(r) Glucose-infused M5
(s) Glucose-infused M5
(t) Glucose-infused M9
(u) Lactate-infused M3
(v) Lactate-infused M4
(w) Lactate-infused M10
(x) Lactate-infused M11
R'_{glc}
Source tissue: Liver
Sink tissue: Heart
Mouse: Glucose-infused M1
(y)
Perturbation of glucose circulatory flux
Sink tissue
GLC
Plasma
Sum
Source tissue
Median R'_{glc}
Perturbation of lactate circulatory flux
LAC
Perturbation of input flux
Source tissue
Value
SUP
Perturbation of MID data
m+0 m+1 m+2 m+3

Figure S9. Results of the basic two-tissue model without physiological constraints on TCA fluxes. Related to STAR Methods.

(a-h) Comparison of experimental and predicted MID in the model. Average of predicted MID in all feasible solutions are displayed. Standard deviation is also displayed as error bar. Because of the low abundance, only isotopomers with more than one 13C are displayed. **(i)** Distribution of 18 variable fluxes in all feasible solutions. Source tissue is liver and sink tissue is heart. **(j-p)** Distribution of cost functions of feasible solutions fitted with different sink tissue and data from different mice, compared with unfitted control data. Source tissue in all fittings is liver. U-statistics of rank-sum test and p-values are displayed. **(r-x)** Distribution of glucose contribution based on the model with different sink tissues fitted with different mice. The orange dash line represents 0.5 threshold. Data set is from glucose-infused mice (M1, M5, M9) and lactate-infused mice (M3, M4, M10, M11) in Hui et al, 2017. Ht: heart, Br: brain, SkM: skeletal muscle, Kd: kidney, Lg: lung, Pc: pancreas, SI: small intestine, Sp: spleen, Uf: data from random unfitted control. **(y)** Parameter sensitivity analysis. Similar with Figure 3, distribution of medians reflects parameter sensitivities for this model. The distribution of medians under perturbation of glucose circulatory flux, lactate circulatory flux, input flux in source tissue and MID data. Most of the medians are above the 0.5 threshold, which implies that under most perturbations, glucose contributes more than lactate to the TCA cycle. Data set is from glucose-infused mouse M1 in Hui et al, 2017. Source tissue is liver and sink tissue is heart.

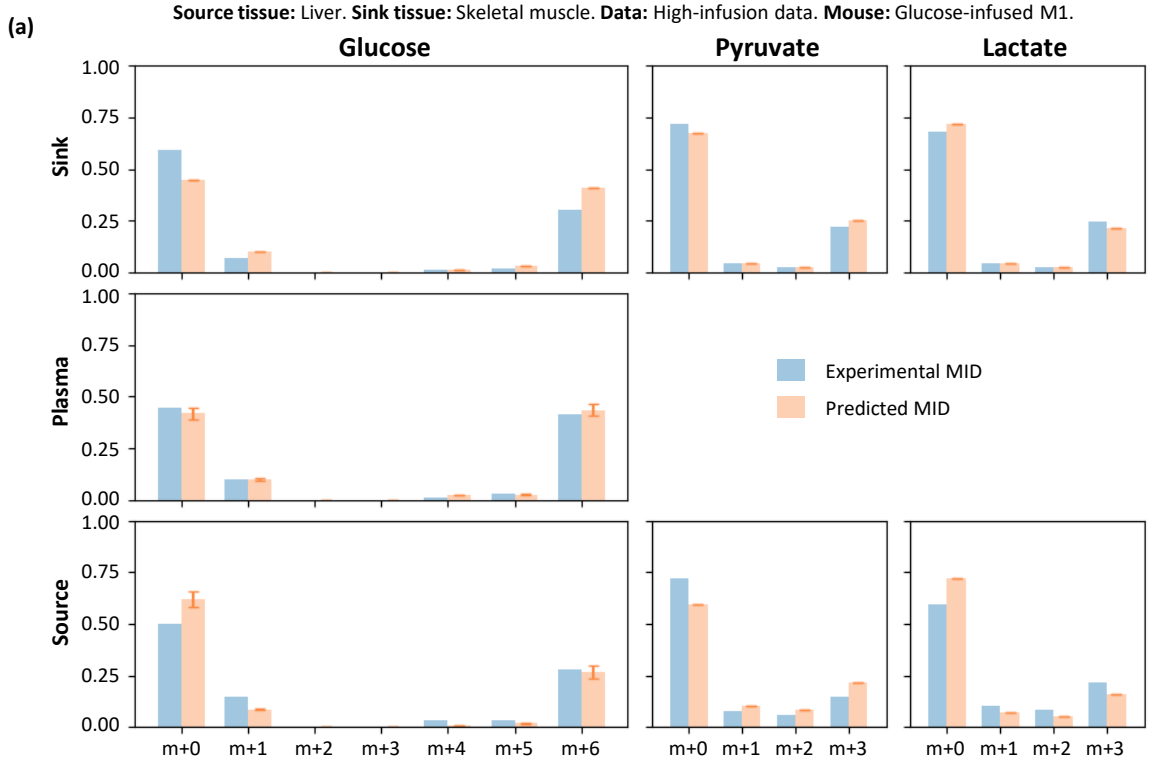

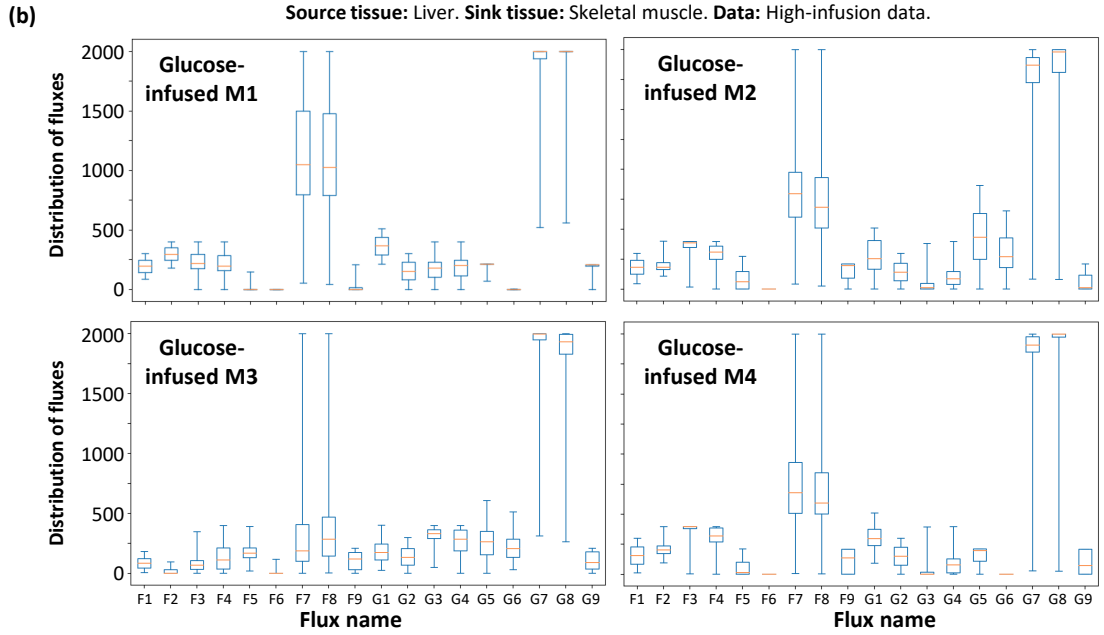

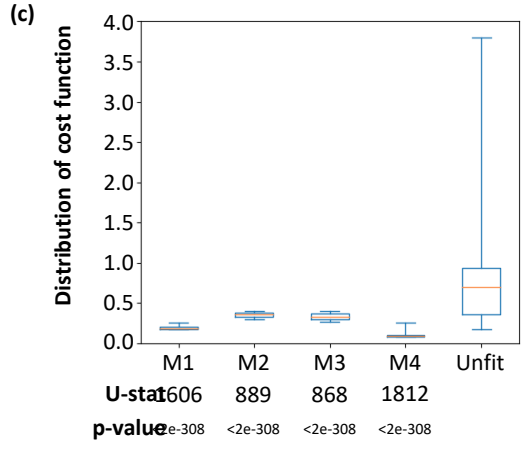

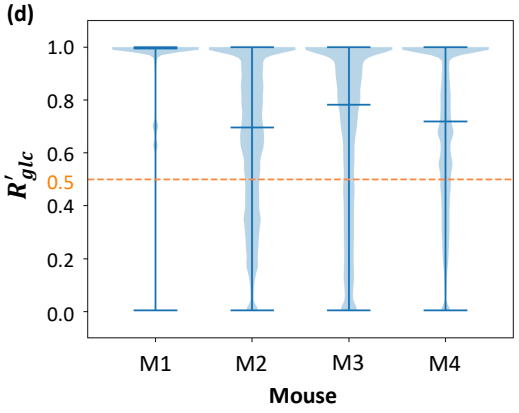

Source tissue: Liver.
Sink tissue: Skeletal muscle.
Data: High-infusion data.

Figure S10. Results of different animal strain and infusion rate without physiological constraints on TCA fluxes. Related to STAR Methods.

(a) Comparison of experimental and predicted MID in the model. Average of predicted MID in all feasible solutions are displayed. Standard deviation is also displayed as error bar. **(b)** Distribution of 18 variable fluxes in all feasible solutions. **(c)** Distribution of cost function fitted with data from different mice or unfitted control data. U-statistics of rank-sum test and p-values are displayed. **(d)** Distribution of glucose contribution shows glucose contributes more than lactate to the TCA cycle. All subfigures are fitted with different glucose-infused mice from the high-infusion data. Source tissue is liver and sink tissue is skeletal muscle. Specifically, subfigure **(a)** is based on data from glucose-infused mouse M1. In all box plots, boxes represent quantiles and whiskers represent extremes.

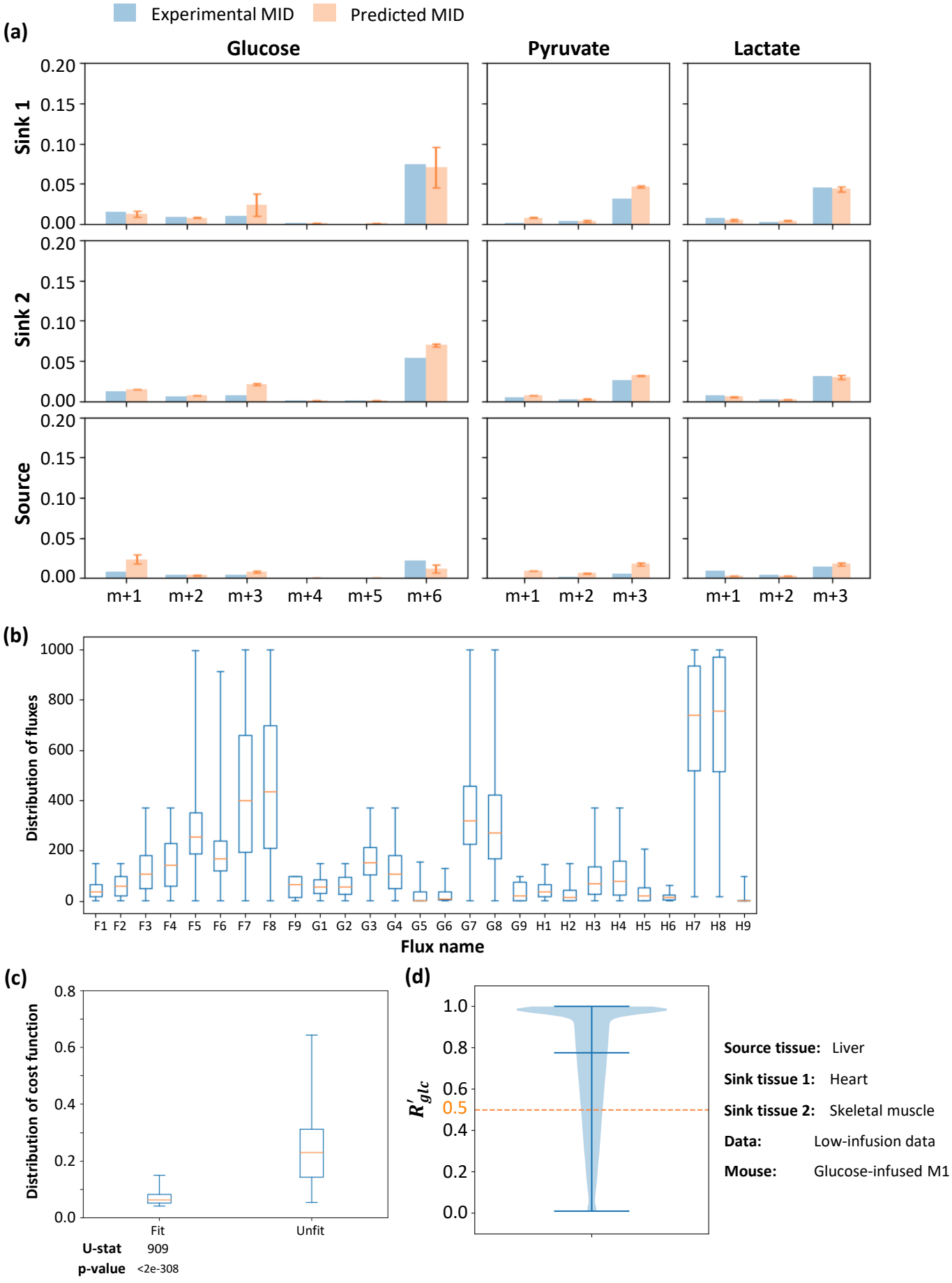
Experimental MID
Predicted MID
(a)
Glucose
Pyruvate
Lactate
Sink 1
Sink 2
Source
0.20
0.15
0.10
0.05
0.00
m+1
m+2
m+3
m+4
m+5
m+6
(b)
Distribution of fluxes
1000
800
600
400
200
0
F1 F2 F3 F4 F5 F6 F7 F8 F9 G1 G2 G3 G4 G5 G6 G7 G8 G9 H1 H2 H3 H4 H5 H6 H7 H8 H9
Flux name
(c)
Distribution of cost function
0.8
0.6
0.4
0.2
0.0
Fit
Unfit
U-stat 909
p-value <2e-308
(d)
R'_{glc}
1.0
0.8
0.6
0.5
0.4
0.2
0.0
Source tissue: Liver
Sink tissue 1: Heart
Sink tissue 2: Skeletal muscle
Data: Low-infusion data
Mouse: Glucose-infused M1

Figure S11. Results across multiple tissues without physiological constraints on TCA fluxes. Related to STAR Methods.

(a) Comparison of experimental and predicted MID in the model. Average of predicted MID in all feasible solutions are displayed. Standard deviation is also displayed as error bar. Because of the low abundance, only isotopomers with more than one 13C are displayed. **(b)** Distribution of 27 variable fluxes in all feasible solutions. **(c)** Distribution of cost functions of feasible solutions compared with that from unfitted control. U-statistics of rank-sum test and p-values are displayed. **(d)** Distribution of glucose contribution shows glucose contributes more than lactate to the TCA cycle. In all subfigures, the model is fitted with glucose-infused mouse M1 from the low-infusion data in Hui et al, 2017. The source tissue is liver and the sink tissue 1 and 2 are heart and skeletal muscle respectively. In all box plots, boxes represent quantiles and whiskers represent extremes.

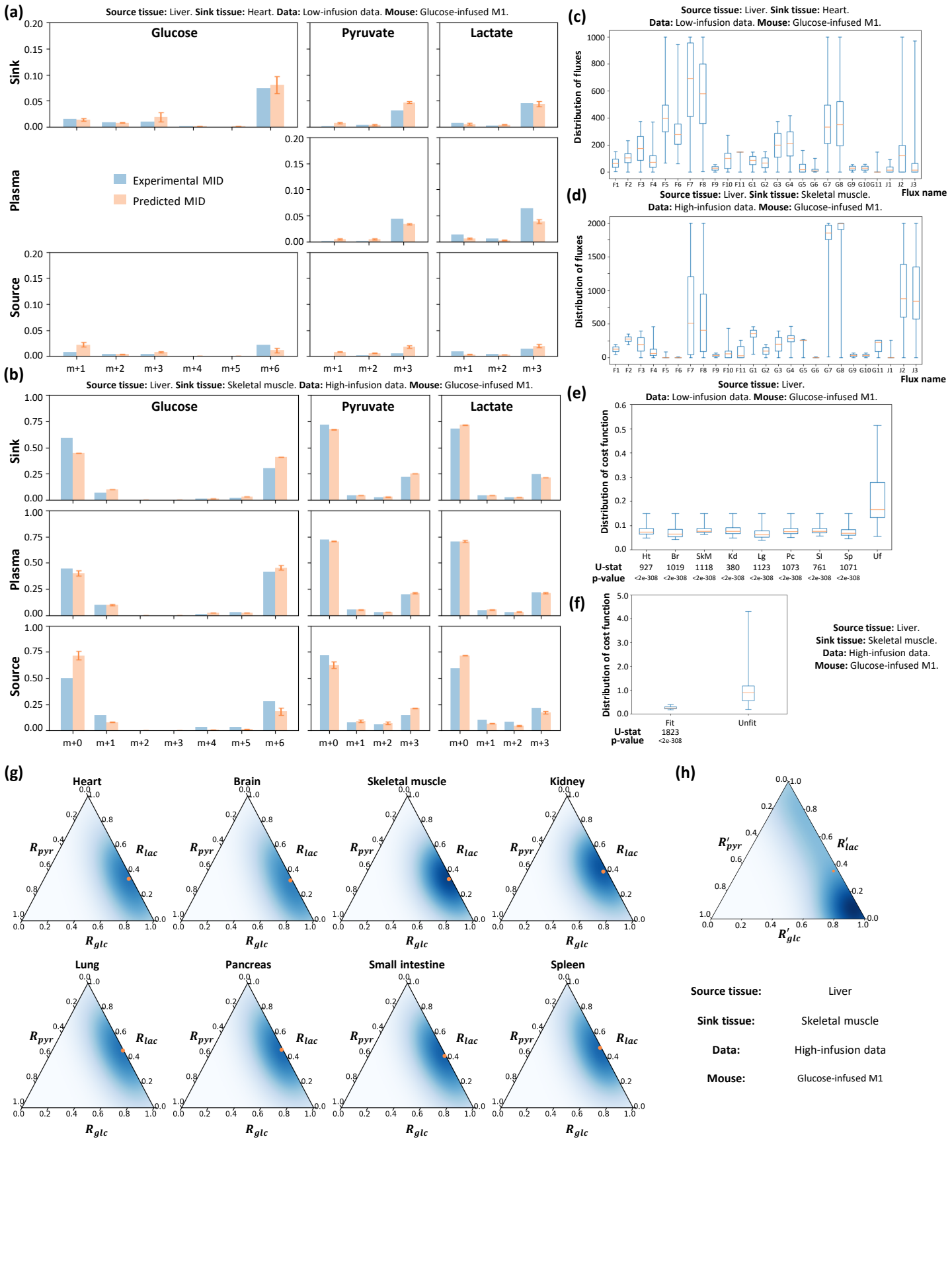
(a)
Source tissue: Liver. Sink tissue: Heart. Data: Low-infusion data. Mouse: Glucose-infused M1.
Glucose
Pyruvate
Lactate
Sink
Plasma
Source
Experimental MID
Predicted MID
m+1
m+2
m+3
m+4
m+5
m+6
(b)
Source tissue: Liver. Sink tissue: Skeletal muscle. Data: High-infusion data. Mouse: Glucose-infused M1.
m+0
(c)
Source tissue: Liver. Sink tissue: Heart.
Data: Low-infusion data. Mouse: Glucose-infused M1.
Distribution of fluxes
F1 F2 F3 F4 F5 F6 F7 F8 F9 F10 F11 G1 G2 G3 G4 G5 G6 G7 G8 G9 G10 G11 J1 J2 J3
Flux name
(d)
Source tissue: Liver. Sink tissue: Skeletal muscle.
Data: High-infusion data. Mouse: Glucose-infused M1.
(e)
Source tissue: Liver.
Data: Low-infusion data. Mouse: Glucose-infused M1.
Distribution of cost function
Ht Br SkM Kd Lg Pc Sl Sp Uf
U-stat 927 1019 1118 380 1123 1073 761 1071
p-value <2e-308
(f)
Fit Unfit
U-stat 1823
p-value <2e-308
Source tissue: Liver.
Sink tissue: Skeletal muscle.
Data: High-infusion data.
Mouse: Glucose-infused M1.
(g)
Heart
Brain
Skeletal muscle
Kidney
Lung
Pancreas
Small intestine
Spleen
R_{pyr}
R_{lac}
R_{glc}
(h)
R'_{pyr}
R'_{lac}
R'_{glc}
Source tissue: Liver
Sink tissue: Skeletal muscle
Data: High-infusion data
Mouse: Glucose-infused M1

Figure S12. Results containing multiple circulating metabolites feeding the TCA cycle without physiological constraints on TCA fluxes. Related to STAR Methods.

(a, b) Comparison of experimental and predicted MID in the model fitted with the low-infusion data **(a)** or the high-infusion data **(b)**. Average of predicted MID in all feasible solutions are displayed. Standard deviation is also displayed as error bar. **(c, d)** Distribution of 25 variable fluxes in all feasible solutions fitted with the low-infusion data **(c)** or the high-infusion data **(d)**. **(e, f)** Distribution of cost functions of feasible solutions compared with that from random unfitted control, fitted with the low-infusion data **(e)** or the high-infusion data **(f)**. U-statistics of rank-sum test and p-values are displayed. **(g, h)** Contributions to the TCA cycle when additional nutrients are considered, fitted with the low-infusion data **(g)** or the high-infusion data **(h)**. The orange point indicates average level.

Subfigure **(a)**, **(c)**, **(e)** and **(g)** are fitted with glucose-infused mouse M1 from the low-infusion data in Hui et al, 2017, and source tissue is liver. Specifically, sink tissue in **(a)** and **(c)** is heart. Subfigure **(b)**, **(d)**, **(f)** and **(h)** are fitted with glucose-infused mouse M1 from the high-infusion data, and the sink tissue and source tissue are liver and skeletal muscle respectively.